# Red-Light-Responsive Polypeptoid Nanoassemblies Containing a Ruthenium(II) Polypyridyl Complex with Synergistically Enhanced Drug Release and ROS Generation for Anticancer Phototherapy

Yandong Ma, Zhihua Zhang, Fan Sun, Pierre Mesdom, Xin Ji, Pierre Burckel, Gilles Gasser, Min-Hui Li

▶ **To cite this version:**

Yandong Ma, Zhihua Zhang, Fan Sun, Pierre Mesdom, Xin Ji, et al.. Red-Light-Responsive Polypeptoid Nanoassemblies Containing a Ruthenium(II) Polypyridyl Complex with Synergistically Enhanced Drug Release and ROS Generation for Anticancer Phototherapy. Biomacromolecules, 2023, 10.1021/acs.biomac.3c00949 . hal-04318192

**HAL Id: hal-04318192**
**https://hal.science/hal-04318192v1**

Submitted on 1 Dec 2023

**HAL** is a multi-disciplinary open access archive for the deposit and dissemination of scientific research documents, whether they are published or not. The documents may come from teaching and research institutions in France or abroad, or from public or private research centers.

L'archive ouverte pluridisciplinaire **HAL**, est destinée au dépôt et à la diffusion de documents scientifiques de niveau recherche, publiés ou non, émanant des établissements d'enseignement et de recherche français ou étrangers, des laboratoires publics ou privés.

# Red-light Responsive Polypeptoid Nano-assemblies Containing a Ruthenium(II) Polypyridyl Complex with Synergistically Enhanced Drug Release and ROS Generation for Anticancer Phototherapy

*Yandong Ma,[a] Zhihua Zhang,[a] Fan Sun,[a] Pierre Mesdom,[b] Xin Ji,[c] Pierre Burckel,[d] Gilles Gasser,[b] Min-Hui Li[a]**

[a] Chimie ParisTech, PSL University, CNRS, Institut de Recherche de Chimie Paris, UMR8247, 75005 Paris, France.

[b] Chimie ParisTech, PSL University, CNRS, Institute of Chemistry for Life and Health Sciences, Laboratory for Inorganic Chemistry, 75005, Paris, France.

[c] Key Laboratory of Biomaterials of Guangdong Higher Education Institutes, Engineering Technology Research Center of Drug Carrier of Guangdong, Department of Biomedical Engineering, Jinan University, Guangzhou 510632, China.

[d] Université Paris-Cité, CNRS, Institut de Physique du Globe de Paris, 75005 Paris, France.

*Email : min-hui.li@chimieparistech.psl.eu

**ABSTRACT**

Polymer micelles/vesicles made of a red-light-responsive Ru(II)-containing block copolymer (PolyRu) are elaborated as a model system for anticancer phototherapy. PolyRu is composed of PEG and a hydrophobic polypeptoid bearing thioether side chains, 40% of which are coordinated with [Ru(2,2′:6′,2″-terpyridine)(2,2′-biquinoline)]$(PF_6)^2$ via Ru-S bond resulting in 67wt% of Ru complex

loading capacity. Red-light illumination induces the photocleavage of Ru-S bond and produces [Ru(2,2′:6′,2″-terpyridine)(2,2′-biquinoline)($H_2O$)]($PF_6$)$_2$. Meanwhile, ROS are generated under the photosensitization of Ru complex and oxidize hydrophobic thioether to hydrophilic sulfoxide, causing the disruption of micelles/vesicles. During the disruption, ROS generation and Ru complex release are synergistically enhanced. PolyRu micelles/vesicles are taken up by cancer cells, while they exhibit very low cytotoxicity in the dark. In contrast, they show much higher cytotoxicity under red-light irradiation. PolyRu micelles/vesicles are promising nano-assembly prototypes that protect metallodrugs in the dark but exhibit light-activated anticancer effects with spatiotemporal control for photoactivated chemotherapy and photodynamic therapy.

**KEYWORDS:** Polymer vesicle, polypeptoid, Ru(II) complex, light-activated cleavage, photoresponsive release, phototherapy

## INTRODUCTION

Polymer nano-assemblies as drug delivery systems have drawn an increasing attention for cancer therapy, since they can circumvent some pharmacological limitations of small molecular medicine such as poor water solubility, nonspecific distribution, systemic toxicity, etc.[1-2] Moreover, stimuli-responsive polymer nano-assemblies further improve the bioavailability of drugs through controllable drug release in response to endogenous stimuli (such as pH variation, redox gradient, enzymes, *etc*)[3-5] or exogenous stimuli (such as light, temperature change, ultrasound, magnetic field, *etc*).[6-10] Among these stimuli, light-responsive drug release systems have been actively studied due to their convenient remote-control and exceptional spatiotemporal resolution.[2] This work aims to construct light-responsive polymer micelles and vesicles based on an amphiphilic polypeptoid containing a Ru(II) complex using red-light as stimulus (Scheme 1). The polypeptoid, composed of *N*- thioether substituted amino acids,[11] is chosen because of its exceptional biocompatibility and biodegradability.[12-13] The Ru(II) complex with cleavable Ru(II)-thioether coordination bond (noted as Ru-S hereinafter) is chosen as prodrug model since Ru-S bond can be cleaved by long-wavelength

lights and the released Ru complex can be used in both photoactivated chemotherapy and photodynamic therapy.[14-18] The long-wavelength lights like red or near-infrared (NIR) light show higher tissue penetration and cause less photodamage to biological systems than UV light frequently reported in light-responsive systems.[19]

Ru(II) complexes bearing terpyridyl-like or other sterically hindered ligands can selectively photo-substitute one of the ligands by solvent molecule(s).[20-21] Such reactivity is explained by their low-lying, metal centered ($^3$MC) excited states with dissociative character, which are thermally populated from the photochemically generated metal-to-ligand charge-transfer ($^3$MLCT) excited states under visible and NIR light illumination. These light-induced substitution reactions have been used as an interesting way to activate caged bioactive ruthenium complexes or ligands both in small molecular systems[22-25, 26] and in polymer self-assembly drug delivery systems.[27, 28-30] The Ru complex used in this work is [Ru(tpy)(biq)($H_2O$)]($FP_6$)$_2$ (Ru = ruthenium, tpy = 2,2′:6′,2″-terpyridine and biq = 2,2′-biquinoline) since it has been reported previously in small molecular systems and in polymer nano-assemblies for anticancer application.[26-27, 31] The different manners to encapsulate Ru complexes into nanomaterials were recently reviewed.[32-35] For example, in reported Ru-containing polymer micelles and vesicles,[27] a non-biodegradable polymethacrylate was used as polymer backbone, to which Ru complexes were coordinated via cyano-groups. Here, biocompatible and biodegradable PEGylated polypeptoid, PEG-*b*-PMeSPG (PEG = poly(ethylene glycol), PMeSPG = poly(N-3-(methylthio)propyl glycine)), [36] with a thioether-bearing polypeptoid PMeSPG is used and [Ru(tpy)(biq)]($PF_6$)$_2$ groups are attached to the hydrophobic block PMeSPG via Ru-S bond. Concretely, [Ru(tpy)(biq)(thioether)]($PF_6$)$_2$ is formed via the exchange reaction between aqua ligand in [Ru(tpy)(biq)($H_2O$)]($PF_6$)$_2$ and thioether ligand in the dark. Nearly 40% of PMeSPG side chains are coordinated with Ru complexes resulting in 67wt% Ru complexes in the final amphiphilic block copolymer PolyRu. Depending on the co-solvent used, PolyRu is self-assembled into micelles and vesicles by nanoprecipitation.

Amphiphilic polypeptoids bearing thioether groups and their polymersomes are oxidation responsive, as demonstrated previously by our group.[36-37] The hydrophobic thioether groups in the hydrophobic polypeptoid block can be transformed into more polar sulfoxide or sulfone groups under the action of oxidants like $H_2O_2$ generated enzymatically or reactive oxygen species (ROS) generated photochemically in the presence of a photosensitizer. Consequently, porous structures appeared in the vesicular membranes and polymersome bursting or disruption occurred eventually, because a part of amphiphilic block copolymers become entirely hydrophilic. Actually, as many Ru complex, $[Ru(tpy)(biq)(L)](PF_6)_2$ (L = $H_2O$ or -S-) is also a photosensitizer that can produce ROS to kill cancer cells in photodynamic therapy (PDT),[15, 38-39] and to also oxidize hydrophobic thioether to hydrophilic sulfoxide. The change of hydrophobic/hydrophilic balance within amphiphilic copolymers then result in the disassembly or dissolution of their nano-assemblies and may synergistically facilitating the Ru complexes release despite the low biological ROS concentration (50 μM – 100 μM).[40, 41]

In this work, the photocleavage of the Ru-S coordination bond and their influence on the PolyRu nano-assemblies were studied. Red-light activated ROS generation and the Ru complexes release synergistically boosted by ROS were investigated. Finally, cellular uptake and cytotoxicity assay of PolyRu micelles and vesicles were performed. Interestingly, although the PEGylation exhibited less non-specific cellular uptake,[42-43] the introduction of Ru complexes in the PEGylated polypeptoid nano-assemblies could increase the cancer cellular uptake. PolyRu micelles and vesicles showed very low cytotoxicity in dark ($IC_{50}$ > 280 μM) and high cytotoxicity under red-light activation ($IC_{50}$ ~ 20 - 30 μM) which was even higher than that of the free aqua Ru complexes ($IC_{50}$ ~ 45 μM). Therefore, PolyRu nano-assemblies reported here represent an interesting prototype for ruthenium-based photoactivated chemotherapy and photodynamic therapy.

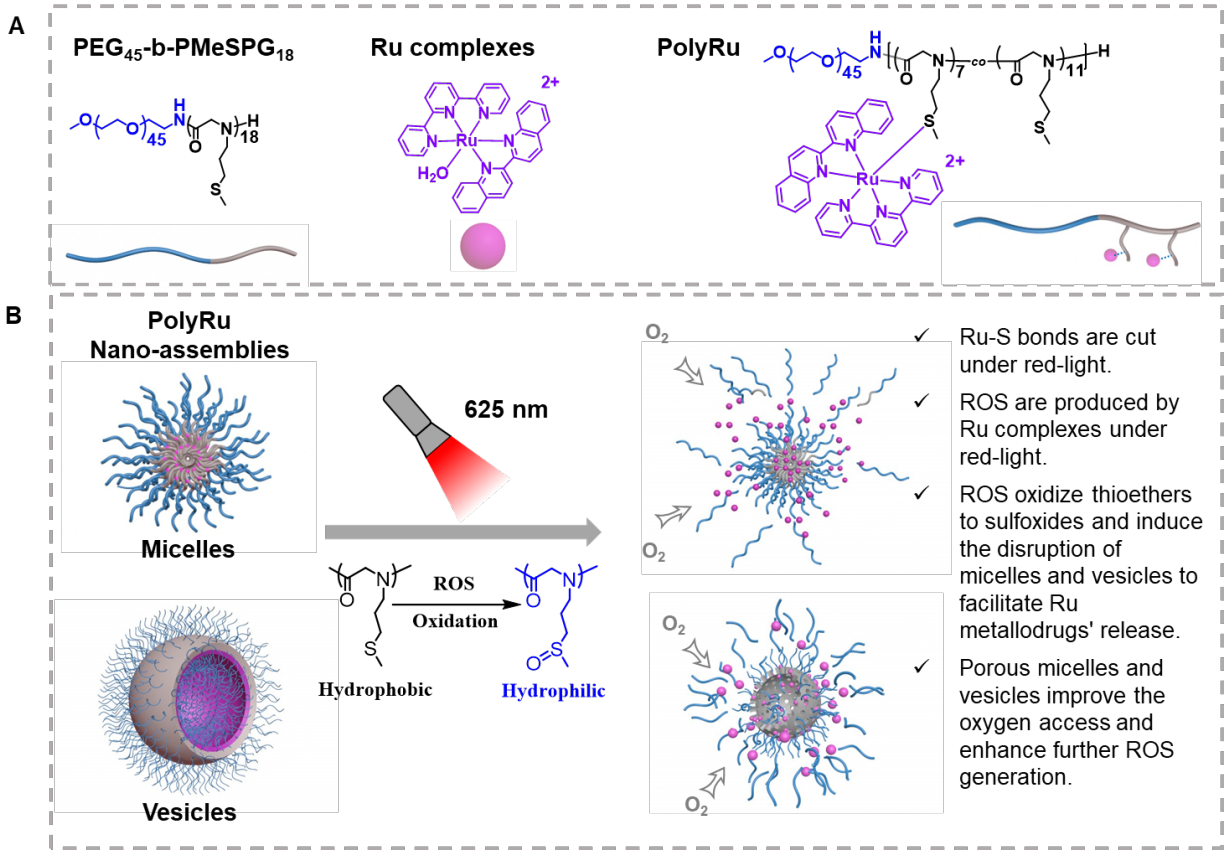


**Scheme 1.** (A) Amphiphilic diblock copolymer PEG-*b*-PMeSPG, Ru complex $[Ru(tpy)(biq)H_2O](PF_6)_2$ and amphiphilic diblock copolymer PolyRu with $[Ru(tpy)(biq)](PF_6)_2$ (Ru = ruthenium, tpy = 2,2′:6′,2″-terpyridine and biq = 2,2′-biquinoline) complexes connected to the hydrophobic block PMeSPG via Ru-S bonds. (B) PolyRu micelles and vesicles illuminated by red-light (625 nm). Light illumination provokes the fracture of coordination bond Ru-S in polypeptoid block. Meanwhile, ROS generated by Ru complexes excited by red-light oxidize the hydrophobic thioether groups to hydrophilic sulfoxide groups; consequently, micelles and vesicles become porous and start to disrupt. Porous micelles and vesicles improve the oxygen access and enhance further ROS generation. The whole process causes rapid release of Ru complexes for anticancer therapy.

## EXPERIMENTAL SECTION

### Synthesis of Ru complex and amphiphilic diblock copolymers PEG-*b*-PMeSPG and PolyRu

$[Ru(tpy)(biq)(H_2O)](PF_6)_2$ was synthesized as reported in the litterature.[27, 20, 44] The monomer N-3-(methylthio)propyl glycine N-thiocarboxyanhydride (MeSPG-NTA) was synthesized according to

our previous work.[37] The polymer PEG-*b*-PMeSPG was prepared by ring opening polymerization of MeSPG-NTA using PEG-$NH_2$ as macro-initiator.[36] The detailed procedures and characterizations are described in the Supporting Information.

To synthesize the Ru complex-functionalized amphiphilic diblock copolymer, PolyRu, PEG-*b*-PMeSPG (35 mg, 0.0075 mmol) and Ru complex $[Ru(tpy)(biq)(H_2O)](PF_6)_2$ (182 mg, 0.2025 mmol) were dissolved into acetone (8 mL) in a 25 mL Schlenk tube. After being degassed for 30 min, the mixture was stirred at room temperature under argon for 72h in the dark. The reaction mixture was participated from ethanol to obtain the crude polymer, which was further purified twice by precipitation using acetone/ethanol as solvent/non-solvent pair. The final polymer was dried in vacuum (68 mg, yield: 85.07%). Its characterization is described in the Supporting Information.

**Self-Assembly of PolyRu and of $PEG_{45}$-*b*-$PMeSPG_{18}$**

PolyRu (2.0 mg) was dissolved in 0.2 mL DMF or 0.2 mL THF/acetone mixture (with different ratio) and stirred for 0.5 h. A total of 1.8 mL of milli-Q water was slowly injected into the solution at a speed of 0.6 mL/min with slight shaking. Then, the colloidal dispersion was further stirred for 0.5 h and dialyzed against Milli-Q water for 8 h to remove organic solvents using a dialysis tube (*M*w cutoff, 3.5 kDa). In the dialysis process, Milli-Q water was replaced approximately every 1 h. The preparation of $PEG_{45}$-*b*-$PMeSPG_{18}$ nanoparticles was conducted in the same way using DMF as organic solvent.

The loading capacity of Ru complex in the polymer nano-assemblies can be calculated by the following equation:

$$\text{Loading capacity (wt\%)} = \frac{\text{Weight of Ru complex in the PolyRu nano-assembly}}{\text{Weight of PolyRu nano-assembly}}$$

**Characterization of Polymer nano-assemblies**

*Dynamic light scattering (DLS).* The hydrodynamic diameters of the self-assembles and their surface Zeta potentials were measured by Zetasizer Nano Series (Malvern Instruments) at 25 °C. For size analysis, the samples were measured at a fixed angle at 90° and a wavelength of 657 nm.

*UV-visible absorbance and spectrofluorometers.* UV spectra were measured by a Milton Ray Spectronic 3000 Array spectrophotometer. Photoluminescence (PL) spectra were collected on a Horiba FluoroMax Spectrofluorometers.

*Attenuated Total Reflection−Fourier transform infrared (ATR-FTIR) spectroscopy.* The measurements were conducted with a Nicolet Magna-IR 550 FTIR spectrometer with 50 scans.

*Scanning electron microscope (SEM).* SEM images were observed by a Zeiss Leo 1530 FEG-SEM. Briefly, the silicon wafers were treated in 100 mL mixture of $H_2SO_4/H_2O_2$ (v/v, 3/1) at 90 °C for 2h. After hydrophilizing, the silicon wafers washed by Milli-Q water, acetone, and ethanol successively, then dried with liquid nitrogen before use. To prepare SEM sample, a drop of dispersion of polymer nano-assemblies was added onto silicon wafer and freeze-dried.

*Transmission electron microscopy (TEM).* The morphology of the polymer nano-assemblies was imaged by a JEOL 2100 Plus transmission electron microscope operated at 200kV. To prepare TEM grid, 5 μL of dispersion of polymer nano-assemblies was added on a carbon-covered 200-mesh holey copper grid (Ted Pella Inc., U.S.A.) and dried under vacuum.

*LED source.* A high intensity LED spotlight with λ = 625 nm (device type: 86-432, Edmund Optics Ltd) was used for all light illumination studies.

**Detection of reactive oxygen species (ROS) and singlet oxygen ($^1O_2$)**

DCFH was used to detect the ROS produced by PolyRu copolymer and PolyRu nano-assemblies. The commercially available DCFH-DA was first activated by NaOH solution to DCFH. DCFH solution (1 μM) was added into $[Ru(tpy)(biq)(H_2O)]^{2+}$ (70 μM) solution, and PolyRu micelles and vesicles aqueous dispersion (containing 70 μM of Ru complexes), respectively. Afterward, the mixtures were irradiated by 625 nm-light (30 $mW/cm^2$) for different length of time. ROS generated could transform non-fluorescent DCFH to hyperfluorescent oxidated DCFH. The fluorescence intensity of the oxidated DCFH (with peak at 521 nm, $\lambda_{ex}$ = 488 nm) was measured as a function of red-light irradiation time.

The $^1O_2$ generated from $[Ru(tpy)(biq)(H_2O)]^{2+}$ and PolyRu copolymer were monitored by the

transformation of fluorescent 1, 3-diphenylisobenzofuran (DPBF) to non-fluorescent oxidized DPBF under red-light irradiation.[38, 45] Briefly, the methanol solution of DPBF (25 μM) in the presence of $[Ru(tpy)(biq)(H_2O)]^{2+}$ (55 μM) and PolyRu copolymer (containing 55 μM of Ru complexes), respectively, was irradiated by red light ($\lambda$ = 625 nm, 30 mW/cm$^2$) for different length of time. The fluorescence intensity (emission around 446 nm, $\lambda_{ex}$ = 405 nm) was subsequently recorded as a function of irradiation time. As a control experiment, the solution of DPBF (25 μM) was irradiated in the same way but without Ru samples.

**Cell uptake, intracellular ROS detection and cytotoxicity assays**

*Cell Culture.* The A549 cell line was incubated in F-12k media (Gibco) supplemented with 10% fetal calf serum (Gibco) and 1% Penicillin-Streptomycin antibiotic (Gibco). Cells were used in the assays one week after the end of the treatment to avoid interfering with the results.

*Cell uptake tests by Inductively Coupled Plasma Mass Spectrometry (ICP-MS).* A549 cells were incubated at a density of 1 × 10$^6$ cells/dish. After 24 h, cells were treated with 10 μM of PolyRu micelles and vesicles as well as 70 μM of Ru complexes (all at 70 μM equivalent concentration of Ru complexes) in the cell culture medium, respectively. Cells were collected after different time of treatment (2 h, 4 h, 6 h and 8 h), counted, and stored at −80 °C. For the analysis by ICP-MS, all cellular samples were digested in 70% $HNO_3$ (0.5 mL, 70 °C, overnight) and subsequently diluted 1:100 (1% HCl solution in Mili-Q water). ICP-MS measurements were performed on an Agilent 7900 Quadrupole ICP-MS located at the Institut de Physique du Globe de Paris (France). The Ru content of each sample was detected using $^{101}$Ru as monitored isotope without collision gas for higher sensitivity. The uncertainties were calculated by error propagation equations, considering the combination of standard deviation (SD) on the replicated samples (n = 3), internal standard ratio and blank subtraction. The amount of metal detected in the cell samples was transformed from ppb to μg o1f metal. Data were then normalized to the number of cells and expressed as nanograms of metal/number of cells.

*Intracellular ROS detection by flow cytometry.* A549 cells (5×10$^5$ cells well-1) were seeded in the 6-

well plates and cultured for 24 h. After treatment with medium alone, Ru complexes, PolyRu micelles and vesicles (70 μM of Ru complexes) for 6 h, the cells were washed with PBS and then incubated with 1 mL fresh medium containing 10 μM dichloro-dihydro-fluorescein diacetate (DCFH-DA) for 30 min at 37 °C. After washing thrice with PBS, the cells were exposed to red light irradiation ($\lambda$ = 625 nm, 11.57 mW/cm$^2$) for 30 min. Subsequently, the cells were trypsinized and collected, and their mean fluorescence was analyzed by flow cytometry ($\lambda_{ex}$ = 488 nm, $\lambda_{em}$ = 525 nm) to evaluate the intracellular ROS level.

*Cytotoxicity Assay in the dark and under red-light irradiation.* The cytotoxicity of Ru complex, PolyRu micelles or PolyRu vesicles was accessed by a fluorometric cell viability assay using Resazurin (Acros Organics). Briefly, A549 cells were seeded in triplicate in 96-well plates at a density of 5×10$^3$ cells/well in 100 μL. After incubation at 37 °C, 5% $CO_2$ for 24 h, the cell medium was replaced by a series of solutions of Ru complex, PolyRu micelles or PolyRu vesicles with increasing concentrations (100 μL/well). Ru complex solution with concentrations from 0.03 μM to 280 μM were diluted with media from 10 mM stock solution of Ru complex in DMSO. PolyRu micelles and vesicles with concentrations from 0.01 μM to 40 μM (polymer PolyRu concentration) were diluted with media from their initial dispersion in water. The cells were then incubated with different Ru samples for 6h. For phototoxicity assay, cells plates were irradiated under red light (625 nm, 11.57 mW/cm$^2$) for 1 h. For dark toxicity assay, cells plates were kept in the dark. After another 24 h of incubation, the medium was removed and 100 μL of complete medium containing resazurin (0.2 mg/mL final concentration) was added in each well. After 4 h of incubation at 37 °C, the fluorescence signal of the resorufin product transformed from resazurin was read (ex 540 nm, em 590 nm) by Infinite 200 PRO Microplate Reader from TECAN. $IC_{50}$ values were then calculated using GraphPad Prism software.

## RESULTS AND DISCUSSION

### Synthesis of amphiphilic block copolymer PolyRu

The synthesis of PolyRu with Ru complexes-coordinated polypeptoid block is shown in Scheme 2. $[Ru(tpy)(biq)(H_2O)](PF_6)_2$ was first synthesized as described in the literature (see SI and Scheme S1, Figure S1 and S2).[27] The block copolymer $PEG_{45}$-*b*-PMeSPG was prepared by the ring-opening polymerization (ROP) of MeSPG-NTA (Figure S3) using amino-terminated $PEG_{45}$-$NH_2$ (molecular weight $M_n$ = 2000 Da and degree of polymerization DP = 45) as a macromolecular initiator according to the procedures published previously.[36] The obtained $PEG_{45}$-*b*-PMeSPG was characterized by $^1H$ NMR and Size Exclusion Chromatography (SEC) (Figure S4, Figure S5 and Table S1), which showed a polymer of $M_n$ = 4.6 kDa with narrow molecular weight distribution ($Đ$ =1.08) corresponding to $PEG_{45}$-*b*-$PMeSPG_{18}$ (DP = 18 for PMeSPG). $[Ru(tpy)(biq)]^{2+}$ was then coordinated with the thioether groups of the PMeSPG block in $PEG_{45}$-*b*-$PMeSPG_{18}$ (ratio Ru/thioether = 1/1) by ligand exchange between aqua and thioether to get PolyRu ($M$n = 10900 Da). The block copolymer PolyRu was finally obtained by precipitating thrice in ethanol to remove unreacted $[Ru(tpy)(biq)(H_2O)](PF_6)_2$. The composition of the final PolyRu was calculated according to the characteristic signals in $^1H$ NMR spectrum (Figure S6). The signal "b" of the $H_{C8}$ in biquinoline spatially close to the coordination bond Ru-S is upfield-shifted compared to the signal "a" of $H_{C8}$ in biquinoline spatially close to Ru-$H_2O$ bond (Figure S6 and S2). However, the signal "a" still co-exists with "b" in the final PolyRu despite the purification, which corresponds approximatively to one free $[Ru(tpy)(biq)(H_2O)](PF_6)_2$ with nine $[Ru(tpy)(biq)(-S-)](PF_6)_2$ connected to PMeSPG, probably because the coordination exchange between Ru-$H_2O$ and Ru-S is a reversible reaction and reaches a certain equilibrium.[20] Evaluation of the percentage of Ru-S coordination in the block copolymer PolyRu was done by comparing the integration of signal "b" to the integration of -$CH_2$-$CH_2$-O- signals of PEG. Only a part of thioester groups is coordinated with $[Ru(tpy)(biq)]^{2+}$; Ru-S percentage is of 39%, namely 7 monomers over 18 per chain being coordinated.

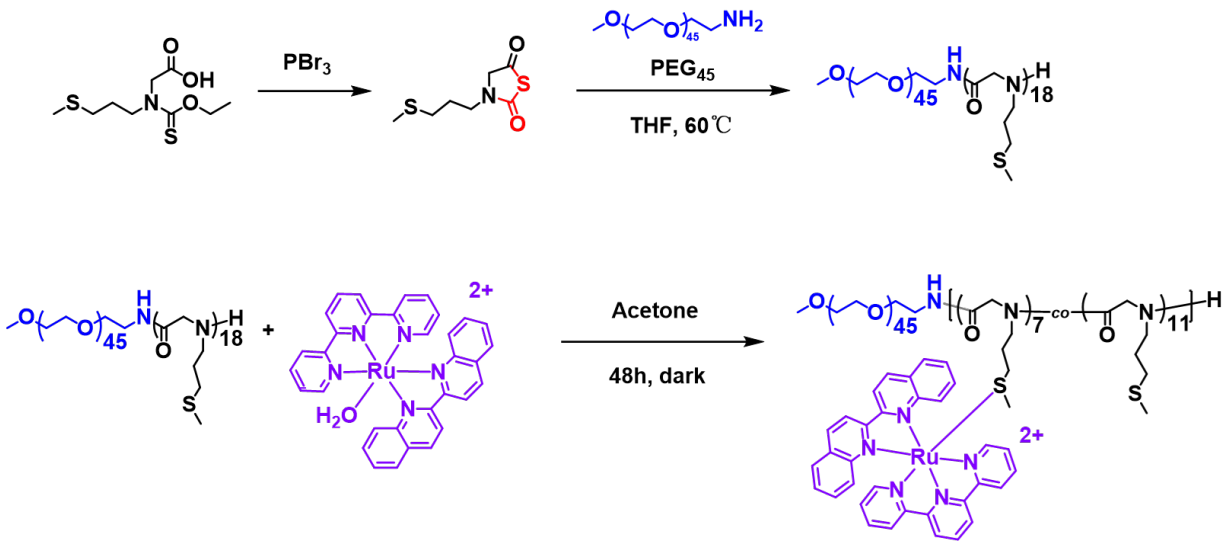


**Scheme 2.** Synthetic route to PEG$_{45}$-*b*-PMeSPG$_{18}$ and Ru complexes-coordinated PEG$_{45}$-*b*-PMeSPG$_{18}$ (PolyRu).

**PolyRu micelles and vesicles self-assembled by nanoprecipitation**

The nano-assemblies of PolyRu were fabricated through nanoprecipitation method. The hydrophilic block PEG weight ratio over the copolymer weight of PolyRu, $f_{PEG}$, is 22%. The control of morphology was achieved by using different organic cosolvent including THF/acetone mixture and DMF. Briefly, PolyRu was first solubilized in the organic solvent at a concentration of 1wt %. To 0.2 mL of this PolyRu solution was added dropwise 1.8 mL Milli-Q water at a rate of 0.2 mL/min with slight shaking. The dispersion was then dialyzed thrice against a large volume of water within 8 h to eliminate the organic solvent. The nano-assemblies were subsequently characterized by transmission electron microscopy (TEM), scanning electron microscopy (SEM), and dynamic light scattering (DLS). The loading capacity of Ru complexes in polymer micelles and vesicles was 67%, which was a relative high value due to the coordination binding of Ru complex to PMeSPG$_{18}$ in PolyRu.

As revealed by SEM images (Figure 1A), micelles were the major morphology of nano-assemblies using DMF as the organic solvent. An average diameter of 13 ± 2 nm was obtained by analysing 30 micelles in the SEM images by ImageJ. By DLS (Figure 1B and Figure S7), an average hydrodynamic diameter ($D_h$) of 21± 1 nm (number profile) was measured. $D_h$ is higher than the

diameter measured by SEM, because DLS gave the hydrodynamic diameter of micelles in hydrated state in water, while SEM measured the diameter of micelles in dried state.

Different ratios of THF/acetone from 0/3 to 3/1 were also tested as organic cosolvent for PolyRu nanoprecipitation. There, THF is a good solvent for $PEG_{45}$-*b*-$PMeSPG_{18}$, but a bad solvent for Ru complex, while acetone is a good solvent for both $PEG_{45}$-*b*-$PMeSPG_{18}$ and Ru complex. No self-assemblies were obtained using pure acetone as cosolvent. Increasing the THF/acetone ratio, the self-assemblies could be detected by DLS, as shown in Figure S8 and Table S2. The average hydrodynamic diameters of self-assemblies increased (from 49 ± 2 nm to 68 ± 1 nm) with the THF/acetone ratio's increasing. Notably, the self-assemblies fabricated using THF/acetone ratio = 1/1 exhibited the narrowest size distribution with PDI of 0.32. Therefore, THF/acetone (1/1) was chosen as organic cosolvent to prepare the self-assemblies for the following investigation. SEM and TEM (Figure 1C and Figure S9A) images reveal the vesicular structures for these PolyRu self-assemblies, where collapsed vesicles with membranes of high contrast are visible. An average hydrodynamic diameter ($D_h$) of 59 ± 2 nm (number profile) with PDI of 0.32 was measured by DLS (Figure 1D and Figure S9B).

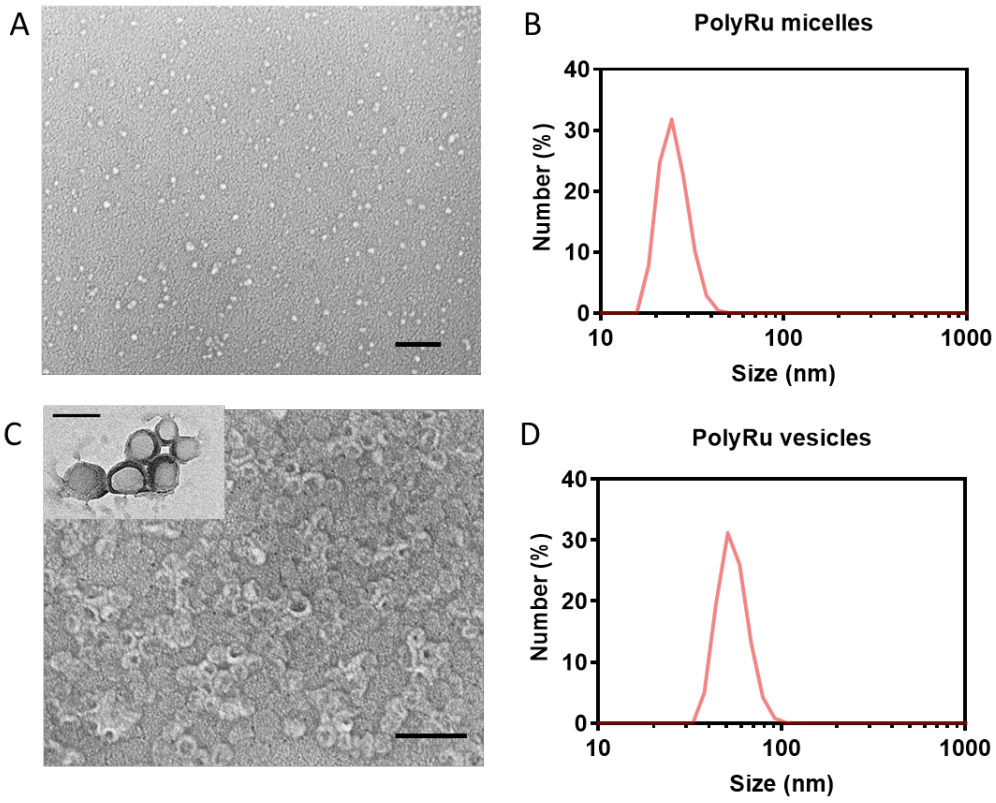


**Figure 1**. Characterization of PolyRu self-assemblies. (A) SEM image of PolyRu micelles formed using DMF as organic cosolvent. Scale bar: 200 nm (B) Size distributions of PolyRu micelles by DLS (number profile). (C) SEM image with TEM image in upper-left inset of PolyRu vesicles formed using THF/acetone = 1/1 as organic cosolvent. Scale bar: 200 nm (SEM) and 100 nm (TEM, upper-left inset) (D) Size distributions of PolyRu vesicles (number profile). For DLS measurement, the concentration of PolyRu micelles or vesicles in water corresponds to 26 μM PolyRu polymers.

**Photocleavage of Ru-S coordination bond in PolyRu and PolyRu nano-assemblies**

Before the study of Ru complex photo-substitution, the stability of PolyRu and PolyRu nano-assemblies in aqueous medium in the dark needs to be first checked. As in the case of Ru complex coordinated with small thioether,[37] the UV-visible spectrum of PolyRu showed a typical metal-to-ligand charge transfer (MLCT) band of Ru-S with maximal absorption around 520 nm while extending to around 700 nm (Figure S10). However, the precursor, $[Ru(tpy)(biq)(H_2O)](PF_6)_2$ with aqua ligand showed the MLCT band of Ru-$H_2O$ with maximal absorption around 550 nm (Figure S10). Therefore, the MLCT band can be used to follow the change of coordination in PolyRu aqueous

solution and in PolyRu nano-assemblies dispersed in the water. As shown in Figure 3A, over 6 h, the MLCT absorption band of PolyRu solution in water/acetone (volume ratio 1/1) shifted from 520 nm to 550 nm with the increase of its intensity, indicating the thermal cleavage of Ru-S band to get uncaged Ru complex with aqua ligand. An equilibrium between Ru-S and Ru-$H_2O$ coordination bonds exists at room temperature. Ru-$H_2O$ can be produced in abundant water environment.[20] Nevertheless, the MLCT band of PolyRu micelles and vesicles dispersed in the water or PBS had no remarkably change over 24 h in the dark (Figure 2B, 2C and S11). These interesting observations indicated that self-assemblies enhanced the stability of Ru moiety in PolyRu copolymer, which can be explained since water cannot easily access the hydrophobic core or layer of polymer colloids. The dark stability of micelles and vesicles is the key point in the construction of photocontrolled drug delivery systems.

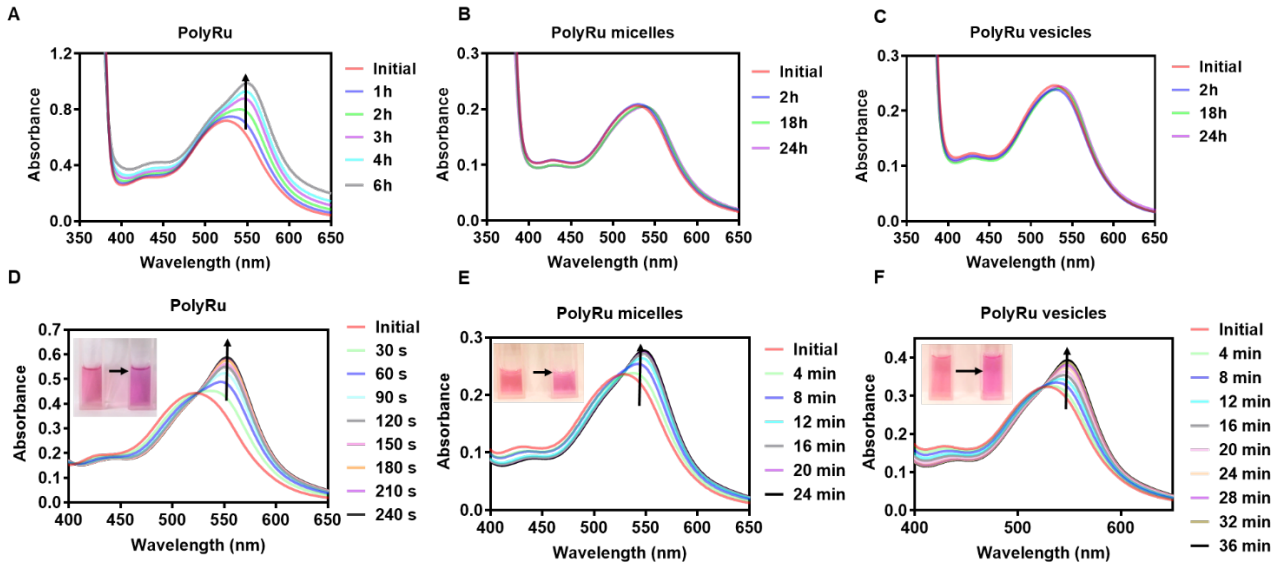


**Figure 2.** (A-C) UV–vis absorption spectra of samples incubated in aqueous solution in the dark for different times. (D-F) UV–vis absorption spectra of samples irradiated under 625 nm light (30 mW/cm$^2$) for different times. (A) amphiphilic block copolymer PolyRu (11 μM) in solution of water/acetone (volume ratio 1/1), (B) PolyRu micelles (9 μM) in water, (C) PolyRu vesicles (9 μM) in water. The inset in (D-F): photographs of samples before (left) and after (right) irradiation.

It is known that the Ru-S bond in the Ru complex-coordinated small thioether molecule can be cleaved in water under visible light to obtain Ru complex with aqua ligand Ru-$H_2O$.[20, 22] Here, this visible light-induced cleavage was first tested for block copolymer PolyRu aqueous solution, then studied in the PolyRu micelles and vesicles, especially for their photo-induced Ru complex release. Interestingly, when 625 nm-light irradiation was applied to PolyRu solution in water/acetone (1/1) mixture (30 mW/cm$^2$, 240 s), the UV-visible spectrum of the solution quickly showed a blue-shifted MLCT band similar to that of Ru-$H_2O$ (Figure 2D and Figure S10). Therefore, a photo-cleavage of Ru-S occurred and photo-induced ligand-substitution took place within 4 min in Ru complex to obtain the uncaged [Ru(tpy)(biq)($H_2O$)]($PF_6$)$_2$. 625 nm light was used since long wavelengths exhibit better tissue penetration compared to short wavelengths.[46] The time evolution of the photo-cleavage was followed every 30 s from 0 to 240 s (Figure 2D) and showed the photo-substitution conversion from Ru-S to Ru-$H_2O$ reached maximum after 210 s (3.5 min) of light illumination (see also Figure S12A). This photo-substitution reaction was also confirmed by $^1$H NMR spectra. As shown in Figure S13, when the irradiation time increased, the signals of the $H_a$ near Ru-$H_2O$ bond at 6.7 ppm increased but those of the $H_b$ near Ru-S bond at 6.37 ppm decreased.

Under 625 nm light irradiation, red shifts of MLCT band were also observed in the UV-visible absorption spectra of PolyRu micelles and vesicles as shown in Figure 2E and 2F. However, the time to reach the maximal conversion took more time in the case of PolyRu micelles ($t_{micelle}$ = 24 min) and vesicles ($t_{vesicle}$ = 36 min) than in the PolyRu polymer solution ($t_{polymer}$ = 3.5 min) (see also Figure S12B and C). These phenomena were also reported in other nano-assemblies made of Ru complex-containing polymer with Ru-cyano (Ru-CN) coordination bonds. [27, 47] Under red-light irradiation (625 nm, 30 mW/cm$^2$), the shift of MLCT band of Ru-CN reached the maximum after $t_{polymer(Ru\text{-}CN)}$ = 2.3 min in block copolymer solution,[47] while in polymer micelles or vesicles (nano-assemblies, NS) it reached the steady state after much longer time ($t_{NS(Ru\text{-}CN)}$ = 180 min). [27] These observations can also be explained by the stabilization effect of nano-assemblies because at the beginning only the Ru-S or Ru-CN at the hydrophilic-hydrophobic interface were in contact with water, and the access of aqua

ligand to the hydrophobic core or membrane was progressive from the hydrophilic-hydrophobic interface. Note interestingly that $t_{NS}/t_{polymer}$ is 78 in the case of Ru-CN polymer nano-assemblies, [27, 47] while $t_{NS}/t_{polymer}$ is only 7 – 10 in PolyRu micelles or vesicles with Ru-S coordination here. The relative photocleavage efficiency of Ru polymer micelles and vesicles with Ru-S coordination is much higher than those with Ru-CN one. This observation is attributed to the simultaneous oxidation of thioether groups by ROS generated in-situ by Ru complexes that are also known as photosensitizer and capable of generating ROS under illumination. The oxidation transformed thioether to sulfoxide and made the hydrophobic block partially or totally hydrophilic. Consequently, the access of water molecules to the Ru-S coordination bonds became easier along with light illumination (see below for details).

**Light-Activated ROS Generation and Boosted Release of Ru complex from PolyRu Micelles and Vesicles**

To assess the ROS generation capacities of PolyRu self-assemblies, DCFH was used as indicator (Figure 3A). The fluorescence of DCFH aqueous solution alone ($\lambda_{ex}$ = 488 nm) was almost negligible after 625 nm-light illumination (30 mW/cm$^2$) of 0 – 24 min, as shown in Figure S14. However, the solution fluorescence exhibited a sharp enhancement with peak around 521 nm as the 625 nm-light illumination time progressed until 24 min in the presence of all samples including Ru complexes, PolyRu micelles and vesicles at an equivalent concentration of Ru of 70 μM, which clearly indicated ROS generation. Moreover, these ROS included $^1O_2$, as confirmed by a separate test in PolyRu organic solution using 1, 3-diphenylisobenzofuran (DPBF) as indicator (see Figure S15 for detail).

Interestingly, after 24 min of irradiation, the emission intensity of DCFH in the presence of PolyRu micelles and vesicles reached twice of that with free Ru complexes (Figure 3B, 3C, 3D and 3E). This observation demonstrated superior ROS production efficiency of PolyRu self-assemblies, which could be associated with the morphological alterations occurring in the PolyRu micelles and vesicles upon irradiation caused by the oxidation of thioether groups. Indeed, the transformation from

thioether groups to sulfoxide groups on PolyRu after irradiation was confirmed by $^{1}$H NMR and ATR-FTIR spectra (see Figure S16 and Figure S13). According to previous works,[37, 48] the oxidization of thioether groups into hydrophilic sulfoxide groups by ROS in the hydrophobic block of PolyRu could provoke the disruption of self-assemblies. Porous structures with higher specific surface area occur in vesicles and micelles during the disruption process, which could improve the oxygen absorption and promote the oxygen contact with the Ru-based photosensitizers to further enhance ROS generation efficiency.[39] Effectively, the disruption of PolyRu micelles and vesicles were followed by their count rate ratio α measured by DLS (α = (derived count rate at the irradiation time t)/(derived count rate at t = 0)), since the derived count rate represented the scattering intensity and demonstrated the size and/or quantities of particles in the solution. The decline of α as a function of irradiation time (Figure 3F) supported the decreasing tendency of concentration/size of the self-assemblies through the photoactivated oxidation.

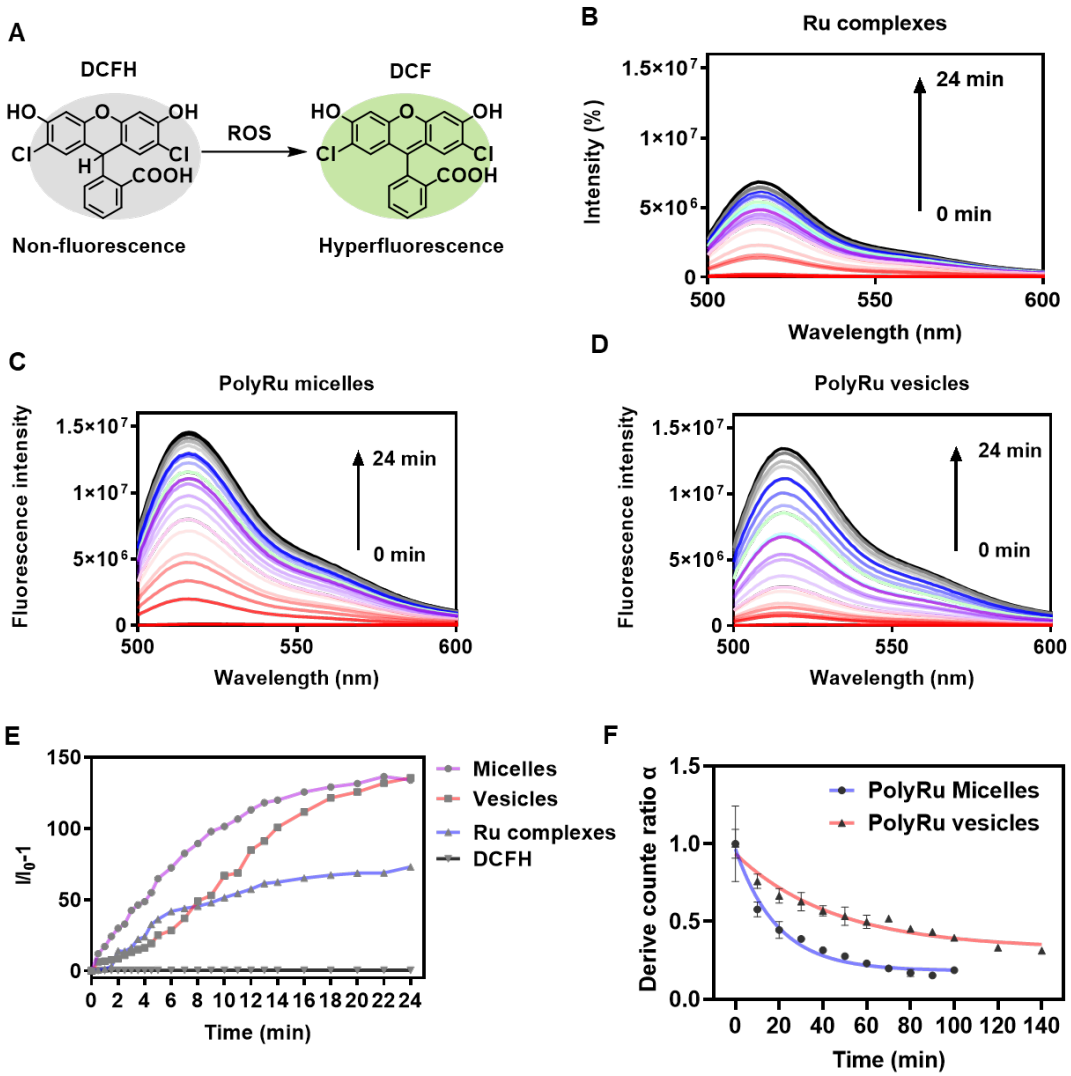


**Figure 3.** ROS generation detected by DCFH for samples under red-light irradiation (625 nm, 30 mW/cm$^2$). (A) ROS transform non-fluorescent DCFH to hyperfluorescent oxidated DCF. The fluorescence increases as a function of time for DCFH aqueous solution, in the presence of Ru complex $[Ru(tpy)(biq)H_2O](PF_6)_2$ (B), in the presence of PolyRu micelles (C), and in the presence of PolyRu vesicles (D). (E) The summary of fluorescence intensity change $(I - I_0)/I_0$ for all samples, $I_0$ being the fluorescence intensity at t = 0 of red-light irradiation. The data of DCFH alone (black) are also shown for reference. (F) The disruption of PolyRu micelles and vesicles traced by count rate ratio. Count rate ratio α = (derived count rate at the irradiation time t)/(derived count rate at t = 0). The symbols are the experimental points. The lines are the fits with the function $\alpha = (\alpha_0 - \alpha_{min})\, e^{-t/\tau} + \alpha_{min}$, where $\alpha_{min}$ = 0.184 (PolyRu micelles) and 0.325 (PolyRu vesicles) correspond to the minimum

count rate ratio nearly unchanged with time, and $\tau$ is the characteristic time when $(\alpha - \alpha_{min})$ declines to 36.8% of $(\alpha_0 - \alpha_{min})$. $\tau$ is 19.05 min for PolyRu micelles, and 45.03 min PolyRu vesicles.

The photoactivated release of Ru complexes from PolyRu self-assemblies under 625 nm-light illumination were then studied *in vitro*.[49] 1 mL of PolyRu micelles or vesicles (1 mg/mL) were irradiated under red-light (625 nm, 30 mW/cm$^2$) for 30 min and then placed into a dialysis bag ($M_w$ cutoff of 3500 Da). The dialysis bag was immersed in 40 mL PBS solution at 37 °C and stirring at 250 rpm, and an aliquot 2mL of the PBS solution was withdrawn after 1 h. The same procedure was performed for the PolyRu micelles and vesicles in the dark without irradiation. The amount of $[Ru(tpy)(biq)(H_2O)](PF_6)_2$ released out of the dialysis bag was $w_{Ru}$ = (40 mL/2 mL)$c_{Ru}$, where the concentration $c_{Ru}$ was determined according to the calibration curve established beforehand using UV-vis spectra (absorbance at 550 nm) (Figure S17 and Table S3). The results showed a relative release $w_{Ru}$(after irradiation)/$w_{Ru}$(in the dark) of 13 and 4 for PolyRu vesicles and micelles, respectively. Clearly, the releases from irradiated samples were significantly higher than those in the dark, because of the photocleavage of Ru-S and the photoactivated disruption of micelles and vesicles through the enhanced ROS generation as discussed above. Interestingly, the difference of the relative light/dark release between micelles and vesicles was not caused by their photoactivated release difference, but by the difference of their background release in the dark (see Table S3). Therefore, PolyRu vesicles are more interesting systems for dark protection and photocontrolled release.

**Cellular Uptake, intracellular ROS detection and Cytotoxicity Assay of PolyRu micelles and vesicles**

In the above sections, we have demonstrated the photocleavage of Ru complexes from PolyRu self-assemblies, ROS generation by PolyRu self-assemblies under red-light irradiation, and the release of Ru complexes promoted by the disruption of PolyRu self-assemblies through the simultaneous ROS generation. The cellular uptake, intracellular ROS generation and cytotoxicity of PolyRu micelles and vesicles were then studied for their potential in anticancer therapy.

PEGylation of anticancer agents has been extensively utilized to prolong their blood circulation time and to enhance their tumor accumulation.[50] However, PEGylation could also reduce their cell uptake due to their nearly neutral surface charge and poor protein adsorption.[42-43] Here, the introduction of Ru complexes might change the situation. The zeta potential of PolyRu micelles and vesicles were first measured as shown in Figure 4A. Effectively, both PolyRu micelles and vesicles exhibited a significant positive surface zeta potential (+16.4 mV for micelles and +18.3 mV for vesicles), in contrast to the zeta potential of +0.96 mV measured for nanoparticles formed by the processor of PolyRu, $PEG_{45}$-*b*-$PMeSPG_{18}$ (Figure S18). According to the litterature,[51-52] the endocytosis of cationic nanoparticles is promoted through the interaction between the positive charge of nanoparticles and the negative charge of cell membrane. The cellular uptakes of PolyRu micelles and vesicles as well as Ru complexes alone were then tested using human non-small cell lung cancer cell line (A549). A549 cells were incubated with PolyRu micelles, PolyRu vesicles or Ru complexes in the cell culture medium, collected at different time (2 h, 4 h, 6 h and 8 h), and digested in 70% $HNO_3$ for analysis by ICP-MS using $^{101}Ru$ as monitored isotopes (see SI for details). As illustrated in Figure 4B, Ru was effectively detected inside the cells, and the intracellular Ru content of both PolyRu micelles and vesicles increased as the incubation time prolonged. Notably, the intracellular Ru content of PolyRu vesicles was approximately twice as much as that of PolyRu micelles, which may be explained by the larger positive zeta potential (+ 18.3 mV, see Figure 6A) and larger size ($D_h$ = 59 nm, see Figure 2) of vesicles. Moreover, the intracellular Ru content of both PolyRu vesicles and micelles were higher than that of Ru complexes alone, which may be caused by the different endocytosis pathway of nanoparticles. Further, the intracellular ROS generation upon red light irradiation was investigated using DCFH-DA. After the diffusion of DCFH-DA into the cell, DCFH-DA is then deacetylated by cellular esterases to the non-fluorescent DCFH, which is later oxidized by ROS into the highly fluorescent DCF (see Figure 3A). The intracellular ROS production is proportional to the fluorescence intensity of DCF measured by flow cytometry (Figure 4C). The results indicated clearly that PolyRu micelles and vesicles produced more ROS inside the cells than

Ru complexes after 30 min of red-light irradiation. Moreover, the mean fluorescence intensity of PolyRu vesicles was higher than that of PolyRu micelles, which could be explained by the more efficient cellular uptake of vesicles compared to micelles (see Figure 4B).

Finally, the cytotoxicity of PolyRu micelles and vesicles was investigated using A549 cells in the dark and under 625 nm light illumination (11.57 mW/cm$^2$, 1 h). The results are summarized in Table 1 (see also Figure S19 and SI for experimental details). As reference, the free Ru complex was first tested with A549 cells in the same conditions. The Ru complex displayed some degree of photo-cytotoxicity and dark-cytotoxicity: the concentration necessary to kill 50% of cancer cells ($IC_{50}$ value) of 68.5 μM in the dark and $IC_{50}$ value of 44.9 μM after irradiation. The photo-cytotoxicity of Ru complexes was higher than that of dark-cytotoxicity because of the photo-generated ROS. As for PolyRu micelles and vesicles, their $IC_{50}$ values in the dark are 280.3 μM and 319.7 μM, respectively, concentrations corresponding to the Ru complexes contents in the nano-assemblies. Therefore, PolyRu micelles and vesicles showed very low cytotoxicity in the dark and the vesicles are still less toxic than micelles. This result is consistent with the protecting role of polymer micelles and vesicles for Ru complexes as above discussed. In contrast, both PolyRu micelles and vesicles exhibited much superior cytotoxicity under red-light irradiation, with $IC_{50}$ values of 27.9 μM and 23.3 μM, respectively, which are even lower than $IC_{50}$ value of free Ru complexes (44.9 μM). This observation could be explained by the higher efficiency of ROS production of PolyRu micelles and vesicles than that of free Ru complexes (see Figure 3E and discussion). The phototoxicity index (PI, defined as the ratio between $IC_{50}$ in the dark and the $IC_{50}$ with light irradiation) of PolyRu micelles (PI = 9.1) and vesicles (PI=13.7) were significantly higher than PI of free Ru complexes (PI = 1.5) (Table 1); moreover, vesicles showed higher photocytotoxicity than micelles. Therefore, PolyRu micelles and vesicles reported here are promising drug delivery systems that can protect Ru complex drugs in the dark and obtain light-activated anticancer effects with spatiotemporal control for photoactivated chemotherapy and photodynamic therapy.

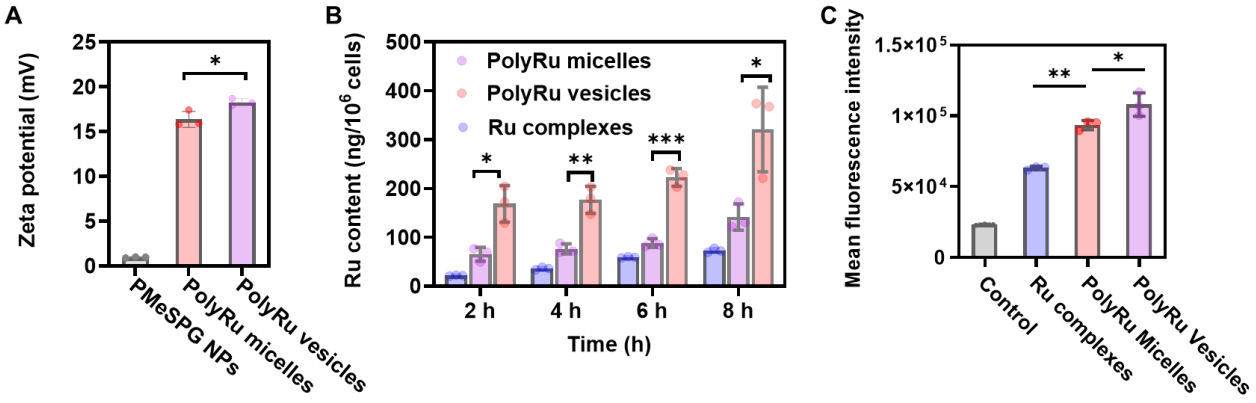


**Figure 4.** (A) Zeta potentials of $PEG_{45}$-*b*-$PMeSPG_{18}$ nanoparticles (PMeSPG NPs), PolyRu micelles and PolyRu vesicles tested by DLS in mili-Q water. (B) Cellular uptake of PolyRu micelles, vesicles, and Ru complexes (all at 70 µM of equivalent concentration of Ru complexes) incubated with A549 cells in various periods (2 h, 4 h, 6 h and 8 h), Ru contents being measured by ICP-MS. (C) Cellular ROS assay by flow cytometry via the measurement of DCF mean fluorescence inside A549 cells ($\lambda_{ex}$ = 488 nm, $\lambda_{em}$ = 525 nm). Cells were incubated with control medium, Ru complexes, PolyRu micelles and vesicles (at 70 µM equivalent concentration of Ru complexes), treated with DCFH-DA, and then irradiate during 30 min by red-light ($\lambda$ = 625 nm, 11.57 mW/cm$^2$). Data are mean ± SD (n = 3). ***P < 0.001, **P < 0.01, *P < 0.05.

**Table 1.** Photo-cytotoxicity and dark cytotoxicity of $[Ru(tpy)(biq)(H_2O)](PF_6)_2$, PolyRu micelles and vesicles incubated with A549 cells

| Compounds | $IC_{50}$ ± SD (µM) | | PI[b] |
|---|---|---|---|
| | Dark | Irradiation[a] | |
| **Ru complexes** | **68.5 ± 1.8** | **44.9 ± 4.5** | **1.5** |
| **PolyRu micelles** | **280.3 ± 19.2** | **27.9 ± 5.1** | **9.1** |
| **PolyRu vesicles** | **319.7 ± 46.9** | **23.3 ± 2.1** | **13.7** |

[a] 625 nm irradiated for 1 h (11.57 mW/cm$^2$) [b] phototoxicity index (PI) defined as the ratio between the concentration necessary to kill 50% of cancer cells ($IC_{50}$) in the dark and the $IC_{50}$ upon light irradiation.

## CONCLUSION

A red-light-responsive amphiphilic block copolymer PolyRu was prepared from PEGylated polypeptoid bearing thioether side chains, PEG-*b*-PMeSPG, and Ru(II) complex, $[Ru(tpy)(biq)(H_2O)](PF_6)_2$. Nearly 40% of PMeSPG side chains were coordinated with Ru complexes resulting in more than 67wt% Ru complexes in the PolyRu. Polymer micelles or vesicles were prepared by nanoprecipitation using either DMF or THF/acetone (1/1) as organic co-solvent. Red-light illumination induced the photocleavage of Ru-S coordination bond and release the Ru complex $[Ru(tpy)(biq)(H_2O)](PF_6)_2$. Meanwhile, Ru complex played the role of photosensitizer and generated ROS *in-situ*, which oxidized the hydrophobic thioether to hydrophilic sulfoxide in the hydrophobic block of PolyRu and caused the disruption of micelles and vesicles. During the disruption of nano-assemblies, the ROS generation was further promoted because of the increased specific hydrophilic/hydrophobic interface area. All these processes synergistically facilitate the release of Ru complex. Furthermore, both PolyRu micelles and vesicles exhibited significant positive surface zeta potentials despite their PEG shell; the presence of coordinated Ru complexes in the core of nano-assemblies did improve their cellular uptake compared to the system without Ru complexes. The cytotoxicity assay showed that both PolyRu micelles and vesicles had very low cytotoxicity in the dark and confirm the protecting role of nano-assemblies for Ru complexes. Interestingly, both PolyRu micelles and vesicles exhibited much higher cytotoxicity under red-light irradiation, with the phototoxicity index PI of 9.1 and 13.7, respectively, in contrast to the PI of free Ru complexes of 1.5. The $IC_{50}$ values of PolyRu micelles and vesicles expressed in concentration of Ru complexes were even lower than $IC_{50}$ value of free Ru complexes because of the enhanced ROS generation efficiency during the disruption of nano-assemblies. Of course, the Ru complex used in this work was not a highly efficient metallodrug for chemotherapy and photodynamic therapy. Other chemical drug could be attached to the Ru complexes[53] and more efficient prodrugs based on other Ru(II) complexes or other thioether ligands like dithioether ligand[22] could be used in the future. In conclusion, PolyRu

vesicles and micelles presented here are promising nano-assembly prototypes that can efficiently protect Ru complex drugs in the dark and achieve red-light-activated anticancer effects with spatiotemporal control for photoactivated chemotherapy and photodynamic therapy.

## ASSOCIATED CONTENT

**Supporting Information**.

The following files are available free of charge.

Materials, and supplemental methods, experimental details, and characterization data (PDF)

## AUTHOR INFORMATION


### Corresponding Author

* Dr. Min-Hui LI : min-hui.li@chimieparistech.psl.eu


### Author Contributions

The manuscript was written through contributions of all authors. All authors have given approval to the final version of the manuscript.

## ACKNOWLEDGMENT


This work is financially supported by the CNRS through the MITI interdisciplinary programs. The Guangzhou Elite Scholarship Council (GESC) and the China Scholarship Council (CSC) are gratefully acknowledged by Yandong Ma and Zhihua Zhang for funding their respective PhD scholarships.


## REFERENCE


1. Mitchell, M. J.; Billingsley, M. M.; Haley, R. M.; Wechsler, M. E.; Peppas, N. A.; Langer, R., Engineering precision nanoparticles for drug delivery. *Nat. Rev. Drug Discovery* **2021,** *20* (2), 101-124.
2. Sun, T.; Zhang, Y. S.; Pang, B.; Hyun, D. C.; Yang, M.; Xia, Y., Engineered nanoparticles for drug delivery in cancer therapy. *Angew. Chem., Int. Ed.* **2014,** *53* (46), 12320-64.
3. Fukino, T.; Yamagishi, H.; Aida, T., Redox-Responsive Molecular Systems and Materials. *Adv. Mater.* **2017,** *29* (25), 1603888.

4. Liu, J.; Huang, Y.; Kumar, A.; Tan, A.; Jin, S.; Mozhi, A.; Liang, X. J., pH-sensitive nano-systems for drug delivery in cancer therapy. *Biotechnol. Adv.* **2014,** *32* (4), 693-710.
5. Mu, J.; Lin, J.; Huang, P.; Chen, X., Development of endogenous enzyme-responsive nanomaterials for theranostics. *Chem. Soc. Rev.* **2018,** *47* (15), 5554-5573.
6. Boissenot, T.; Bordat, A.; Fattal, E.; Tsapis, N., Ultrasound-triggered drug delivery for cancer treatment using drug delivery systems: From theoretical considerations to practical applications. *J. Controlled Release* **2016,** *241*, 144-163.
7. Gohy, J. F.; Zhao, Y., Photo-responsive block copolymer micelles: design and behavior. *Chem. Soc. Rev.* **2013,** *42* (17), 7117-29.
8. Liu, D.; Sun, J., Thermoresponsive Polypeptoids. *Polymers (Basel)* **2020,** *12* (12), 2973.
9. Tombacz, E.; Turcu, R.; Socoliuc, V.; Vekas, L., Magnetic iron oxide nanoparticles: Recent trends in design and synthesis of magnetoresponsive nanosystems. *Biochem. Biophys. Res. Commun.* **2015,** *468* (3), 442-53.
10. Uppalapati, D.; Boyd, B. J.; Garg, S.; Travas-Sejdic, J.; Svirskis, D., Conducting polymers with defined micro- or nanostructures for drug delivery. *Biomaterials* **2016,** *111*, 149-162.
11. Gangloff, N.; Ulbricht, J.; Lorson, T.; Schlaad, H.; Luxenhofer, R., Peptoids and Polypeptoids at the Frontier of Supra- and Macromolecular Engineering. *Chem. Rev.* **2016,** *116* (4), 1753-802.
12. Li, A.; Zhang, D., Synthesis and Characterization of Cleavable Core-Cross-Linked Micelles Based on Amphiphilic Block Copolypeptoids as Smart Drug Carriers. *Biomacromolecules* **2016,** *17* (3), 852-61.
13. Ulbricht, J.; Jordan, R.; Luxenhofer, R., On the biodegradability of polyethylene glycol, polypeptoids and poly(2-oxazoline)s. *Biomaterials* **2014,** *35* (17), 4848-61.
14. Bonnet, S., Why develop photoactivated chemotherapy? *Dalton Trans.* **2018,** *47* (31), 10330-10343.
15. Knoll, J. D.; Turro, C., Control and utilization of ruthenium and rhodium metal complex excited states for photoactivated cancer therapy. *Coord. Chem. Rev.* **2015,** *282-283*, 110-126.
16. Liu, J.; Lai, H.; Xiong, Z.; Chen, B.; Chen, T., Functionalization and cancer-targeting design of ruthenium complexes for precise cancer therapy. *Chem. Commun.* **2019,** *55* (67), 9904-9914.
17. Mahmud, K. M.; Niloy, M. S.; Shakil, M. S.; Islam, M. A., Ruthenium Complexes: An Alternative to Platinum Drugs in Colorectal Cancer Treatment. *Pharmaceutics* **2021,** *13* (8), 1295.
18. Mari, C.; Pierroz, V.; Ferrari, S.; Gasser, G., Combination of Ru(ii) complexes and light: new frontiers in cancer therapy. *Chem. Sci.* **2015,** *6* (5), 2660-2686.
19. Wu, C.; Wu, Y.; Zhu, X.; Zhang, J.; Liu, J.; Zhang, Y., Near-infrared-responsive functional nanomaterials: the first domino of combined tumor therapy. *Nano Today* **2021,** *36*, 100963.
20. Bahreman, A.; Limburg, B.; Siegler, M. A.; Bouwman, E.; Bonnet, S., Spontaneous formation in the dark, and visible light-induced cleavage, of a Ru-S bond in water: a thermodynamic and kinetic study. *Inorg. Chem.* **2013,** *52* (16), 9456-69.
21. Laemmel, A.-C.; Collin, J.-P.; Sauvage, J.-P., Efficient and Selective Photochemical Labilization of a Given Bidentate Ligand in Mixed Ruthenium(II) Complexes of the Ru(phen)2L2+ and Ru(bipy)2L2+ Family (L = Sterically Hindering Chelate). *Eur. J. Inorg. Chem.* **1999,** *1999* (3), 383-386.
22. Meijer, M. S.; Bonnet, S., Diastereoselective Synthesis and Two-Step Photocleavage of Ruthenium Polypyridyl Complexes Bearing a Bis(thioether) Ligand. *Inorg. Chem.* **2019,** *58* (17), 11689-11698.
23. Goldbach, R. E.; Rodriguez-Garcia, I.; van Lenthe, J. H.; Siegler, M. A.; Bonnet, S., N-Acetylmethionine and Biotin as Photocleavable Protective Groups for Ruthenium Polypyridyl Complexes. *Chem. - Eur. J.* **2011,** *17* (36), 9924-9929.
24. Howerton, B. S.; Heidary, D. K.; Glazer, E. C., Strained Ruthenium Complexes Are Potent Light-Activated Anticancer Agents. *J. Am. Chem. Soc.* **2012,** *134* (20), 8324-8327.
25. Wachter, E.; Heidary, D. K.; Howerton, B. S.; Parkin, S.; Glazer, E. C., Light-activated ruthenium complexes photobind DNA and are cytotoxic in the photodynamic therapy window. *Chem. Commun.* **2012,** *48* (77), 9649-9651.

26. van Rixel, V. H. S.; Ramu, V.; Auyeung, A. B.; Beztsinna, N.; Leger, D. Y.; Lameijer, L. N.; Hilt, S. T.; Le Dévédec, S. E.; Yildiz, T.; Betancourt, T.; Gildner, M. B.; Hudnall, T. W.; Sol, V.; Liagre, B.; Kornienko, A.; Bonnet, S., Photo-Uncaging of a Microtubule-Targeted Rigidin Analogue in Hypoxic Cancer Cells and in a Xenograft Mouse Model. *J. Am. Chem. Soc.* **2019,** *141* (46), 18444-18454.
27. Sun, W.; Parowatkin, M.; Steffen, W.; Butt, H. J.; Mailander, V.; Wu, S., Ruthenium-Containing Block Copolymer Assemblies: Red-Light-Responsive Metallopolymers with Tunable Nanostructures for Enhanced Cellular Uptake and Anticancer Phototherapy. *Adv. Healthcare Mater.* **2016,** *5* (4), 467-73.
28. Sun, W.; Li, S.; Haupler, B.; Liu, J.; Jin, S.; Steffen, W.; Schubert, U. S.; Butt, H. J.; Liang, X. J.; Wu, S., An Amphiphilic Ruthenium Polymetallodrug for Combined Photodynamic Therapy and Photochemotherapy In Vivo. *Adv. Mater.* **2017,** *29* (6), 1603702.
29. Chen, M.; Gong, N.; Sun, W.; Han, J.; Liu, Y.; Zhang, S.; Zheng, A.; Butt, H. J.; Liang, X. J.; Wu, S., Red-Light-Responsive Metallopolymer Nanocarriers with Conjugated and Encapsulated Drugs for Phototherapy Against Multidrug-Resistant Tumors. *Small* **2022,** *18* (27), e2201672.
30. Zeng, X.; Wang, Y.; Huang, Y. S.; Han, J.; Sun, W.; Butt, H. J.; Liang, X. J.; Wu, S., Amphiphilic Metallodrug Assemblies with Red-Light-Enhanced Cellular Internalization and Tumor Penetration for Anticancer Phototherapy. *Small* **2022,** *18* (52), e2205461.
31. Askes, S. H. C.; Bahreman, A.; Bonnet, S., Activation of a Photodissociative Ruthenium Complex by Triplet–Triplet Annihilation Upconversion in Liposomes. *Angew. Chem., Int. Ed.* **2013,** *53* (4), 1029-1033.
32. Karges, J., Encapsulation of Ru(II) Polypyridine Complexes for Tumor-Targeted Anticancer Therapy. *BME Front.* **2023,** *4*, 0024.
33. Soliman, N.; Gasser, G.; Thomas, C. M., Incorporation of Ru(II) Polypyridyl Complexes into Nanomaterials for Cancer Therapy and Diagnosis. *Adv. Mater.* **2020,** *32* (47), 2003294.
34. Villemin, E.; Ong, Y. C.; Thomas, C. M.; Gasser, G., Polymer encapsulation of ruthenium complexes for biological and medicinal applications. *Nat. Rev. Chem.* **2019,** *3* (4), 261-282.
35. Zeng, L.; Gupta, P.; Chen, Y.; Wang, E.; Ji, L.; Chao, H.; Chen, Z. S., The development of anticancer ruthenium(ii) complexes: from single molecule compounds to nanomaterials. *Chem. Soc. Rev.* **2017,** *46* (19), 5771-5804.
36. Deng, Y.; Chen, H.; Tao, X.; Trépout, S.; Ling, J.; Li, M.-H., Synthesis and self-assembly of poly(ethylene glycol)-block-poly(N-3-(methylthio)propyl glycine) and their oxidation-sensitive polymersomes. *Chin. Chem. Lett.* **2020,** *31* (7), 1931-1935.
37. Deng, Y. W.; Chen, H.; Tao, X. F.; Cao, F. Y.; Trepout, S.; Ling, J.; Li, M. H., Oxidation-Sensitive Polymersomes Based on Amphiphilic Diblock Copolypeptoids. *Biomacromolecules* **2019,** *20* (9), 3435-3444.
38. Albani, B. A.; Pena, B.; Leed, N. A.; de Paula, N. A.; Pavani, C.; Baptista, M. S.; Dunbar, K. R.; Turro, C., Marked improvement in photoinduced cell death by a new tris-heteroleptic complex with dual action: singlet oxygen sensitization and ligand dissociation. *J. Am. Chem. Soc.* **2014,** *136* (49), 17095-101.
39. Zhang, W.; Li, B.; Ma, H.; Zhang, L.; Guan, Y.; Zhang, Y.; Zhang, X.; Jing, P.; Yue, S., Combining Ruthenium(II) Complexes with Metal-Organic Frameworks to Realize Effective Two-Photon Absorption for Singlet Oxygen Generation. *ACS Appl. Mater. Interfaces* **2016,** *8* (33), 21465-71.
40. Wang, K.; Yang, B.; Ye, H.; Zhang, X.; Song, H.; Wang, X.; Li, N.; Wei, L.; Wang, Y.; Zhang, H.; Kan, Q.; He, Z.; Wang, D.; Sun, J., Self-Strengthened Oxidation-Responsive Bioactivating Prodrug Nanosystem with Sequential and Synergistically Facilitated Drug Release for Treatment of Breast Cancer. *ACS Appl. Mater. Interfaces* **2019,** *11* (21), 18914-18922.
41. Dai, L.; Yu, Y.; Luo, Z.; Li, M.; Chen, W.; Shen, X.; Chen, F.; Sun, Q.; Zhang, Q.; Gu, H.; Cai, K., Photosensitizer enhanced disassembly of amphiphilic micelle for ROS-response targeted tumor therapy in vivo. *Biomaterials* **2016,** *104*, 1-17.
42. Schottler, S.; Becker, G.; Winzen, S.; Steinbach, T.; Mohr, K.; Landfester, K.; Mailander, V.; Wurm, F. R., Protein adsorption is required for stealth effect of poly(ethylene glycol)- and poly(phosphoester)-coated nanocarriers. *Nat. Nanotechnol.* **2016,** *11* (4), 372-7.

43. Zhang, Z.; Chen, H.; Wang, Y.; Zhang, N.; Trepout, S.; Tang, B. Z.; Gasser, G.; Li, M. H., Polymersomes with Red/Near-Infrared Emission and Reactive Oxygen Species Generation. *Macromol. Rapid Commun.* **2023,** *44* (4), e2200716.
44. Boyer, J. L.; Polyansky, D. E.; Szalda, D. J.; Zong, R.; Thummel, R. P.; Fujita, E., Effects of a proximal base on water oxidation and proton reduction catalyzed by geometric isomers of [Ru(tpy)(pynap)(OH2)]2+. *Angew. Chem., Int. Ed.* **2011,** *50* (52), 12600-4.
45. Cheng, Y.; Doane, T. L.; Chuang, C. H.; Ziady, A.; Burda, C., Near infrared light-triggered drug generation and release from gold nanoparticle carriers for photodynamic therapy. *Small* **2014,** *10* (9), 1799-804.
46. Mallidi, S.; Anbil, S.; Bulin, A. L.; Obaid, G.; Ichikawa, M.; Hasan, T., Beyond the Barriers of Light Penetration: Strategies, Perspectives and Possibilities for Photodynamic Therapy. *Theranostics* **2016,** *6* (13), 2458-2487.
47. Chen, M.; Sun, W.; Kretzschmann, A.; Butt, H. J.; Wu, S., Nanostructured polymer assemblies stabilize photoactivatable anticancer ruthenium complexes under physiological conditions. *J. Inorg. Biochem.* **2020,** *207*, 111052.
48. Vasdekis, A. E.; Scott, E. A.; O'Neil, C. P.; Psaltis, D.; Hubbell, J. A., Precision intracellular delivery based on optofluidic polymersome rupture. *ACS Nano* **2012,** *6* (9), 7850-7.
49. He, M.; He, G.; Wang, P.; Jiang, S.; Jiao, Z.; Xi, D.; Miao, P.; Leng, X.; Wei, Z.; Li, Y.; Yang, Y.; Wang, R.; Du, J.; Fan, J.; Sun, W.; Peng, X., A Sequential Dual-Model Strategy Based on Photoactivatable Metallopolymer for On-Demand Release of Photosensitizers and Anticancer Drugs. *Adv. Sci. (Weinh)* **2021,** *8* (23), e2103334.
50. Gref, R.; Domb, A.; Quellec, P.; Blunk, T.; Müller, R. H.; Verbavatz, J. M.; Langer, R., The controlled intravenous delivery of drugs using PEG-coated sterically stabilized nanospheres. *Adv. Drug Delivery Rev.* **2012,** *64*, 316-326.
51. Donahue, N. D.; Acar, H.; Wilhelm, S., Concepts of nanoparticle cellular uptake, intracellular trafficking, and kinetics in nanomedicine. *Adv. Drug Delivery Rev.* **2019,** *143*, 68-96.
52. Hald Albertsen, C.; Kulkarni, J. A.; Witzigmann, D.; Lind, M.; Petersson, K.; Simonsen, J. B., The role of lipid components in lipid nanoparticles for vaccines and gene therapy. *Adv. Drug Delivery Rev.* **2022,** *188*, 114416.
53. Sun, W.; Wen, Y.; Thiramanas, R.; Chen, M.; Han, J.; Gong, N.; Wagner, M.; Jiang, S.; Meijer, M. S.; Bonnet, S.; Butt, H.-J.; Mailänder, V.; Liang, X.-J.; Wu, S., Red-Light-Controlled Release of Drug-Ru Complex Conjugates from Metallopolymer Micelles for Phototherapy in Hypoxic Tumor Environments. *Adv. Funct. Mater.* **2018,** *28* (39), 1804227.

**Red-light Responsive Polypeptoid Nano-assemblies Containing a Ruthenium(II) Polypyridyl Complex with Synergistically Enhanced Drug Release and ROS Generation for Anticancer Phototherapy**

*Yandong Ma,[a] Zhihua Zhang,[a] Fan Sun,[a] Pierre Mesdom,[b] Xin Ji,[c] Pierre Burckel,[d] Gilles Gasser,[b] Min-Hui Li[a]**

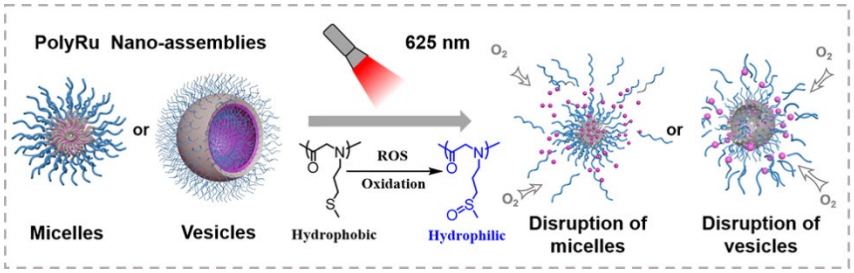


**For Table of Contents Use Only**